

See discussions, stats, and author profiles for this publication at: <https://www.researchgate.net/publication/262844051>

μ High Resolution–Magic–Angle Spinning NMR Spectroscopy for Metabolic Phenotyping of *Caenorhabditis elegans*

ARTICLE in ANALYTICAL CHEMISTRY · JUNE 2014

Impact Factor: 5.64 · DOI: 10.1021/ac501208z · Source: PubMed

CITATIONS

6

READS

66

6 AUTHORS, INCLUDING:



[Alan Wong](#)

French National Centre for Scientific Research

65 PUBLICATIONS 1,401 CITATIONS

[SEE PROFILE](#)



[Florence Solari](#)

Claude Bernard University Lyon 1

30 PUBLICATIONS 621 CITATIONS

[SEE PROFILE](#)



[Benedicte Elena-Herrmann](#)

Ecole normale supérieure de Lyon

54 PUBLICATIONS 1,654 CITATIONS

[SEE PROFILE](#)

μ High Resolution-Magic-Angle Spinning NMR Spectroscopy for Metabolic Phenotyping of *Caenorhabditis elegans*

Alan Wong,^{*,†} Xiaonan Li,^{†,||} Laurent Molin,[‡] Florence Solari,[‡] Bénédicte Elena-Herrmann,[§] and Dimitris Sakellariou^{*,†}

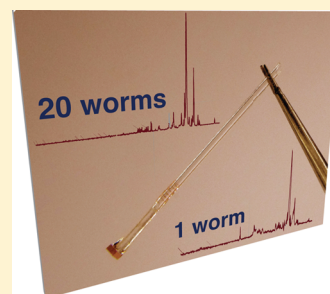
[†]CEA Saclay, DSM, IRAMIS, UMR CEA/CNRS 3299–NIMBE, Laboratoire Structure et Dynamique par Résonance Magnétique, F-91191, Gif-sur-Yvette Cedex, France

[‡]Centre de Génétique et de Physiologie Moléculaires et Cellulaires, UMR CNRS 5534, Université Claude Bernard Lyon 1, Bâtiment Gregor Mendel, 16 Rue Raphaël Dubois, F-69622 Villeurbanne Cedex, France

[§]Centre de RMN à Très Hauts Champs, Institut des Sciences Analytiques, CNRS/ENS Lyon/UCB Lyon-1, Université de Lyon, 5 Rue de la Doua, 69100 Villeurbanne, France

Supporting Information

ABSTRACT: Analysis of model organisms, such as the submillimeter-size *Caenorhabditis elegans*, plays a central role in understanding biological functions across species and in characterizing phenotypes associated with genetic mutations. In recent years, metabolic phenotyping studies of *C. elegans* based on ¹H high-resolution magic-angle spinning (HR-MAS) nuclear magnetic resonance (NMR) spectroscopy have relied on the observation of large populations of nematodes, requiring labor-intensive sample preparation that considerably limits high-throughput characterization of *C. elegans*. In this work, we open new platforms for metabolic phenotyping of *C. elegans* mutants. We determine rich metabolic profiles (31 metabolites identified) from samples of 12 individuals using a ¹H NMR microprobe featuring high-resolution magic-angle coil spinning (HR-MACS), a simple conversion of a standard HR-MAS probe to μ HR-MAS. In addition, we characterize the metabolic variations between two different strains of *C. elegans* (wild-type vs *slcf-1* mutant). We also acquire a NMR spectrum of a single *C. elegans* worm at 23.5 T. This study represents the first example of a metabolomic investigation carried out on a small number of submillimeter-size organisms, demonstrating the potential of NMR microtechnologies for metabolomics screening of small model organisms.



Today, there are many analytical tools available for metabolomics studies,¹ which investigate chemical pathways involving small molecules (metabolites) in biosystems such as biofluids and biopsies. Among them, ¹H NMR spectroscopy offers a quantitative, nondestructive, and high-throughput analytical platform with minimal sample preparation and interference. Thus, NMR is widely used in metabolomics providing a robust metabolic profiling tool to discriminate samples of different biological status or origin.^{2,3} In particular, the use of ¹H NMR spectroscopy has now emerged as a powerful analytical component for investigation of intact biopsies,^{4–6} thanks to the application of ¹H-detected HR-MAS. This technique consists in spinning the sample rapidly at an angle of 54.74° with respect to the static magnetic field B_0 to overcome magnetic field heterogeneities responsible for broad resonance lines that, in the absence of MAS, reduce the spectral information. Hence, ¹H HR-MAS NMR is considered a near universal technique for providing unbiased and high-precision fingerprints of abundant metabolites in intact biological tissues, which has led toward a concept of real-time metabolic profiling of a surgical human biopsy in the clinical practice.^{7,8} In recent reports, Elena-Herrmann and co-workers^{9–11} have demonstrated its potential for metabotyping of intact *Caenorhabditis elegans* worms. These studies have paved a new platform for

NMR-based metabolomics application to submillimeter-size organisms. However, since NMR is an inherently insensitive technique, HR-MAS analysis relies on large sample volume detection (typically corresponding to individual samples of more than 1000 worms). For this reason, the current HR-MAS NMR studies of *C. elegans* involve particularly labor-intensive sample preparation for the biologists. Meanwhile, sampling a large quantity of worms, which is necessary to record sufficient signal, implies that interindividual metabolic variability is averaged offering a global view of the metabolomics phenotype for a population of nematodes. Analysis of small numbers of worms would not only ease the sample preparation but could also allow for individual metabolic screening, opening new possibilities to characterize the phenotypic diversity within genotypes that is not achievable when working with large populations of worms.

There are numerous approaches for improving NMR sensitivity that is represented by the signal-to-noise ratio $SNR \propto (1/V_{noise})[\omega_0^2(B_1/i)]$, where V_{noise} is the total noise received

Received: April 3, 2014

Accepted: May 22, 2014

Published: May 22, 2014

from the coil and sample, ω_0 is the Larmor frequency, and B_1/i is the radio frequency (rf) field per unit current.¹² The simplest is to carry out NMR experiment at high ω_0 , which is proportional to the static magnetic field B_0 . Currently, the highest persistent B_0 of NMR quality is 23.5 T.¹³ Another option is to increase the mass-sensitivity (SNR per unit mass) by miniaturizing the rf receiver coil (i.e., μ coil) to enhance the B_1/i efficiency.¹² The current advanced μ coil technology has led to a near complete liquid-state NMR assignment of a 68-residue protein using only 6 μ L of 1.4 mM of protein.¹⁴ Despite this, μ coil detection under MAS conditions for the study of heterogeneous biosamples is still very limited. This is due to the challenges of assembling a μ coil that is suitable for rapid sample spinning at the magic-angle. Two strategies are currently available. The first consists of a stationary μ coil^{15,16} placed at the magic-angle while the sample is spinning (up to 110 kHz with a 750- μ m μ coil diameter) to suppress spin interactions such as chemical shift anisotropy and dipolar interactions. However, no metabolomics studies have been reported using this strategy. This is probably attributed to the imperfect averaging of the magnetic susceptibility across the stationary μ coil stator. The second option consists of an ensemble of an inductively coupled μ coil resonator spinning together with the sample at the magic-angle.¹⁷ The technique is denoted as the magic-angle coil spinning (MACS). The ensemble spinning allows suppressing magnetic susceptibility broadening from both the μ coil and the sample offering good spectral resolution for biopsies (0.05 ppm).^{17,18} The improved high-resolution (HR)-MACS setup is capable of offering spectral resolution up to 0.002 ppm,¹⁹ which is sufficient for high-precision metabolomic studies.

The present study capitalizes on the new development of HR-MACS, permitting for the first time NMR-based metabolic profiling of a small number of *C. elegans* worms ranging from 10 to 100. This is a dramatic enhancement in mass-sensitivity applications compared to the conventional HR-MAS NMR spectroscopy^{9,10} and mass spectrometry,^{20,21} in which the latter requires about 300 worms in order for an efficient extraction.²⁰ Moreover, we explore the notion of NMR detection of a single *C. elegans* nematode by coupling a small HR-MACS resonator with the highest available B_0 field maximizing both B_1/i and ω_0^2 contributions in sensitivity.

■ EXPERIMENTAL DETAILS

***Caenorhabditis elegans* Strains, Culture Conditions, and Sample Preparation.** Wild-type Bristol N2 and *slcf-1(tm2258)*^{11,22} strains were cultured at 20 °C on nematode growth media (NGM) agar plates freshly poured and seeded with *E. coli* OP50 culture. For worm amplification and synchronization, ten adult worms per plate were allowed to lay eggs for 2–3 h at 20 °C then removed, in order to obtain around 100 progenies per plate. Subsequently, 10 plates corresponding to about 1000 worms are necessary for sampling one NMR data. Three days later worms were recovered and washed 5 times in M9 buffer, separated by 15 s centrifugations at 3000 rpm, in order to get rid of eggs and residual bacteria. Worms were then fixed for 45 min in 1% paraformaldehyde and then washed 5 times in distilled water followed by 5 washes in deuterium oxide.

HR-MACS Resonator Fabrication. Each HR-MACS resonator was constructed by manually winding 8 to 10 turns of a 30 μ m round copper wire around a quartz capillary with a 840/600- μ m, a 550/400- μ m, or a 400/300- μ m in outer/inner

diameter. This forms a solenoid length of about 1.3–1.5 mm with detection volumes of a few hundred nanoliters. Each solenoid was soldered to a nonmagnetic 1.6 or 2.2 pF capacitor (American Technical Ceramics) to give a target ^1H frequency at 800 or 1000 MHz within $\pm 10\%$. The resultant coil quality factors (without sample) are in the range of 40–60. The resonator was secured in a custom-made Kel-F insert that fits tightly inside a ZrO 4 mm Bruker rotor.

Sample-Filling. Sample filling for HR-MACS was performed under a stereomicroscope. The *C. elegans* nematodes were pipetted along with D_2O into the solenoid region of the quartz capillary using a micropipet with a 20 μ L GELoader tip (Eppendorf). Gentle centrifugation was applied to ensure that all worms displace to the solenoid region. The capillary was then sealed with hot paraffin wax and epoxy to prevent leakage during the sample spinning. The worm population was counted under the stereomicroscope during the pipetting procedure. To minimize sample degradation, the entire sample preparation procedure was restricted to <15 min.

For preparation of HR-MAS samples, a pellet of about 10 mL of worms, which corresponds to an estimated quantity of ~ 1000 worms, was transferred into a commercial Bruker disposable Kel-F insert. The pellet was suspended in D_2O and the total effective sample volume was 30 mL. The sealed insert was placed into a MAS rotor.

^1H HR-MACS and HR-MAS NMR Spectroscopy. NMR experiments were carried out on a Bruker Avance spectrometer operating at 800 MHz ($B_0 = 18.8$ T) with a standard Bruker 4 mm HR-MAS probe equipped with a ^2H lock-channel or on a 1000 MHz (23.5 T) Bruker Avance spectrometer with a Bruker 3.2 mm HCN CP-MAS probe equipped with an external ^2H -locking channel. The MAS frequency was adjusted manually using a Bruker pneumatic unit with stability of ± 1 Hz. All acquisitions were recorded under a ^2H -lock. The sample temperature was regulated at 293 K. ^1H chemical shifts were internally referenced to the alanine $-\text{CH}_3-$ doublet at $\delta = 1.47$ ppm.

For nanoliter HR-MACS detection, the HR-MACS resonator is inductively coupled with a MAS probe, converting the HR-MAS probe to a nanovolume capable HR-MAS microprobe. Prior to the acquisition of *C. elegans*, the B_0 shimming was performed on a sucrose- D_2O sample with HR-MACS under slow MAS and checked regularly. The 90° -pulse was calibrated for each HR-MACS resonator to evaluate the coil sensitivity performance compared to the coupled MAS probe, ($B_1^{\text{MACS}}/B_1^{\text{MAS}}$) at a given rf power. To obtain high spectral resolution, slow MAS frequencies below 500 Hz are used;¹⁹ therefore, an 8-step 2D-PASS sequence²³ with water suppression was applied to record sidebands- and water-free spectra. At 18.8 T, the PASS experiment was carried out with an rf power of 1.14 W and with a 1 s recycle delay. A total of 40 960 data points was acquired using a spectral width of 16 025 Hz. At 23.5 T, the experiment was performed with a 0.44 W rf with a recycle delay of 1.25 s and with 65 536 data points using a spectral width of 29 762 Hz. The lower rf power used at 23.5 T is attributed to the fact that a greater B_1/i efficiency is achieved with a smaller resonator,¹² where a 400- μ m (μ coil diameter) HR-MACS resonator is used at 23.5 T as compared to 550- and 840- μ m resonators at 18.8 T.

For HR-MAS detection, the B_0 shimming was performed on a full 4 mm rotor of a 1% CHCl_3 solution in acetone- d_6 to obtain a ^1H line width of 10 Hz (full width at the height of ^{13}C satellites). A ^1H 1D NOESY experiment was carried out for

Table 1. Summary of the NMR Performances of the Acquired ^1H Spectra

worm population	B_0 / T	MAS/ ± 1 Hz	HR-MACS ^a D μm : V ηL	Rel MSE ^b	time/min	SNR ^c	fwhm ^d / ± 0.2 Hz	J -splitting ^d / $\pm 1\%$
1000+	18.8	4000			14	487	8.9	87
12	18.8	314	550: \sim 250	5.2	150	24	8.4	97
10	23.5	357	400: \sim 100	8.4	132	21	18	\sim 5
1	23.5	343	400: \sim 100	10.6	900	14	\sim 45	\sim 2
50 ± 20 ($n = 15$) ^e	18.8	300	840: \sim 250	4.0	166	26 ± 6	9.8 ± 0.2	87 ± 4

^aHR-MACS's diameter and detection volume. ^bThe relative mass-sensitivity enhancement of HR-MACS is determined based on the reciprocity principle¹² by comparing the B_1 field of the HR-MACS coil with the corresponding coupled MAS probe ($B_1^{\text{HRMACS}}/B_1^{\text{MAS}}$) at a given rf power. The variant in MSE is mainly contributed to the difference in the quality factor and tuned-frequency of the resonator. ^cSignal-to-noise ratio (SNR) is determined from the metabolites region 3–4 ppm. ^dThe full width at half-maximum (fwhm) and the J -splitting depth are determined from the alanine doublet at 1.47 ppm. These values were determined prior to a 0.3 Hz line-broadening exponential apodization. ^eNMR discrimination study: the spectra are recorded using a single sample-exchangeable HR-MACS resonator and shown in Figure S3 in the Supporting Information. The listed values are the "mean \pm standard derivation" from the 15 replicate samples.

efficient water suppression using a mixing time of 100 ms, a 90° -pulse of $6.55 \mu\text{s}$ (with 18 W), a 1.7 s recycle delay, and a MAS frequency of 4000 Hz. A total of 44 870 data points were acquired using a spectral width of 16 025 Hz. The spectral NMR performances acquired with the different approaches, HR-MACS and HR-MAS, are summarized in Table 1.

Multivariate Data Analysis. Prior to the analysis, spectra were phased and baseline corrected with exponential apodization of LB = 0.5 Hz using the Bruker interface Topspin 3.0. The spectra were also reduced into 0.002 ppm-wide buckets over the spectral region between -1 and 10 ppm, with exclusion of the water region (4.7 – 5.0 ppm), and normalized by the total sum of intensities using the AMIX interface (Bruker Biospin GmbH). Principal component analysis (PCA) and orthogonal partial least-squares-discriminant analysis (OPLS-DA) were performed to check the data homogeneity, identify the latent patterns, and distinguish worm strains using SIMCA-P 13 (Umetrics, Umea, Sweden).

RESULTS

^1H NMR Spectral Comparison between HR-MACS and HR-MAS. Figure 1 displays the comparison of the metabolic ^1H NMR resonance profiles of *C. elegans* between a 12-worms sample detected with HR-MACS (red spectrum) and \sim 1000 worms with HR-MAS (blue spectrum) experiments at 18.8 T. The worms are cultivated from the same batch to minimize sample discrepancy. Despite the lower SNR in the HR-MACS spectrum, it is obvious that the overall ^1H spectral profiles detected by the two methods are remarkably similar, both in terms of spectral resolution and metabolite content. In fact, the spectral resolution from HR-MACS is slightly better: the alanine doublet at 1.47 ppm exhibits a 97% J -splitting depth compared to 87% from HR-MAS. This is attributed to the ease of achieving homogeneous B_0 fields by shimming over a small-volume sample.²⁴ Impressively, the HR-MACS spectrum reveals a total of 31 metabolites from a sample population of just 12 worms in a near 2 h acquisition. Without HR-MACS, it would require an acquisition time 25 times longer (i.e., 5-fold enhancement, $B_1^{\text{MACS}}/B_1^{\text{MAS}} = 5$) in order to obtain the same SNR. Table S1 in the Supporting Information presents the full list of metabolites identified from the HR-MACS and HR-MAS spectra. We note that the lower SNR in HR-MACS prevents from identifying a few low abundance metabolites detected by HR-MAS. Another spectral difference is that the HR-MACS presents a slightly stronger intensity of the lipids resonances. This is a consequence of the presence of aliphatic protons in the thin layer of glue coated on the μ coil or the epoxy used to

seal the sample inside the sample capillary (see Figure S1 in the Supporting Information); however, these narrow and weak background signals do not interfere the assessments of the neighboring resonances.

Toward ^1H HR-MACS NMR Detection of a Single *C. elegans* Nematode. To explore the possibility of single worm detection, we maximized the ω_0 and B_1/i contributions in SNR by carrying out NMR detection at an ultrahigh field (23.5 T), using coupling with a small HR-MACS resonator (400- μm). Figure 2 shows the ^1H HR-MACS spectra of (a) 10 and (b) 1 *C. elegans* individuals. Because of the inductive coupling with a CP-MAS probe, the resultant spectral resolution is rather low. For example, the J -splitting of the β -glucose doublet-of-doublets at 3.9 ppm is not visible. This lack of resolution arises from the large susceptibility gradients from the MAS stator inside the CP-MAS probe, which is not designed for optimal ^1H high-resolution acquisition. Despite the poor resolution, low abundance metabolites such as choline moieties (3.2 ppm), glucose (3.2–4.0 ppm), tyrosine (6.9, 7.2 ppm), and phenylalanine (7.4 ppm) are clearly identifiable, even in the spectrum of a single worm (Figure 2b). Unfortunately, the lengthy 15 h acquisition of the latter spectrum has resulted in sample degradation and thus led to an increase in metabolite intensities in the δ region of 3–4 ppm. Blaise et al.¹⁰ have reported similar observations after sample spinning at 3500 Hz for 4 h. We believe that using a smaller HR-MACS resonator (i.e., 100- μm) with a ^1H -optimized HR-MAS probe would improve the sensitivity and resolution for a single-worm NMR detection. The spectrum presented here represents the first glimpse of a single submillimeter-scale organism NMR detection.

^1H HR-MACS NMR Discrimination Analysis of Two *C. elegans* Strains. To explore the potential of NMR-based metabolomic studies based on HR-MACS detection, we recorded ^1H HR-MACS NMR spectra at 18.8 T of two *C. elegans* strains: young adult wild-type worms and young adult worms that carry a mutation in the *slcf-1* gene enhancing the lifespan.^{11,21} Replicate samples were recorded for each strain. To ensure the spectral data reproducibility, a single sample-exchangeable HR-MACS resonator (840- μm) was used to record all ^1H NMR spectra (see Figure S2 in the Supporting Information for the description of the sample-exchangeable HR-MACS resonator and its demonstrative study on spectral data reproducibility performance). The ^1H NMR spectra were recorded on samples of 50 ± 20 worms under a slow MAS frequency of 300 Hz (Figure S3a in the Supporting Information) and submitted to multivariate statistical analyses

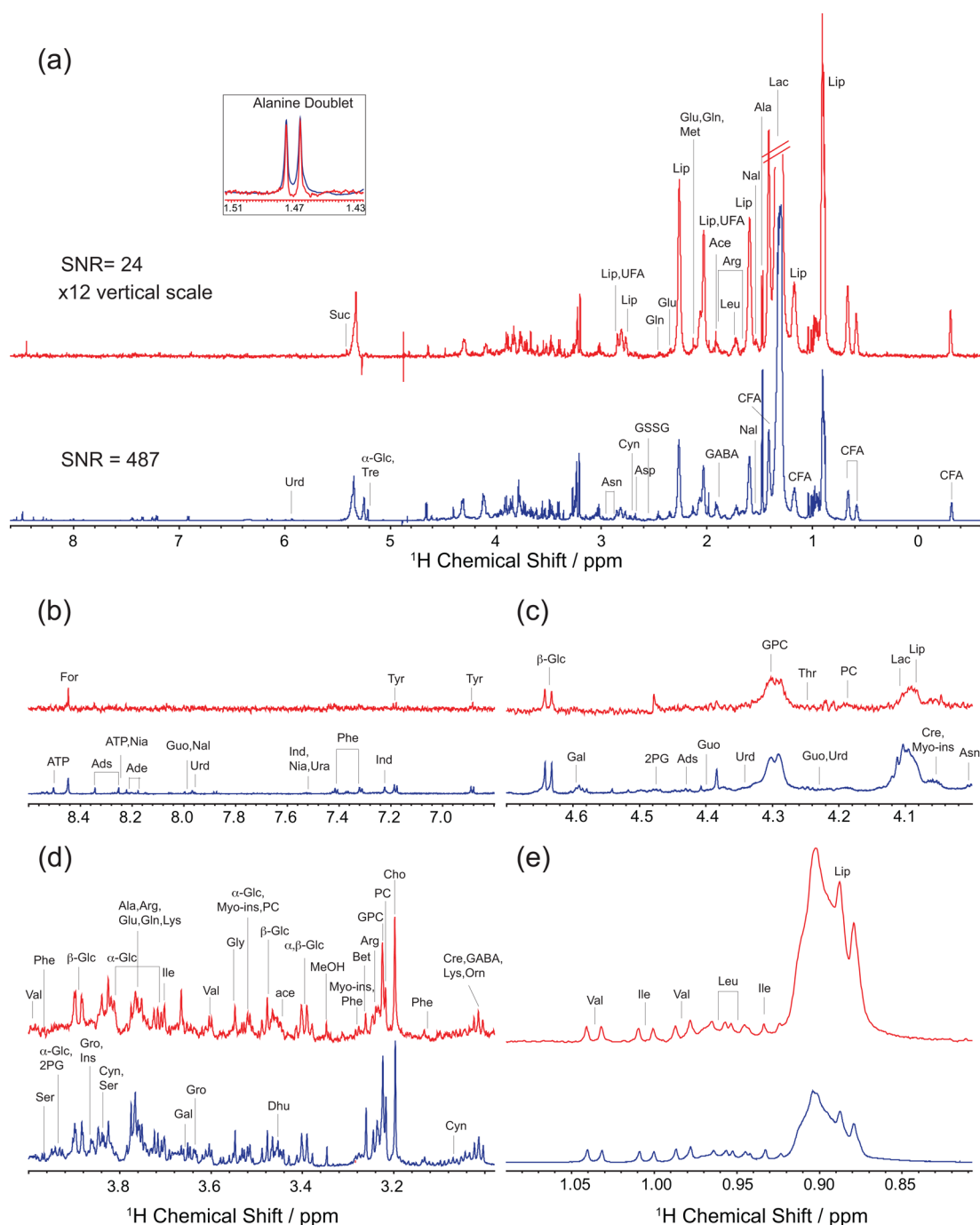


Figure 1. ^1H NMR spectra of *C. elegans* at 18.8 T. (a) A spectral comparison between HR-MACS and HR-MAS NMR detections of *C. elegans*: (red) ^1H spectrum of 12 worms acquired with HR-MACS, with vertical scale amplified by 12; (blue) ^1H spectrum of 1000 worms with HR-MAS. The MAS frequency was set to (red) 314 Hz and (blue) 4000 Hz. The SNR of the metabolite resonances of the chemical shift region 3–4 ppm are found to be (red) 24 and (blue) 487. The insert represents the alanine doublet at 1.47 ppm and is normalized for spectral resolution comparison. The J -splitting depth is found to be about (red) 97% and (blue) 87%. (b–e) The chemical shift expansions showing the detailed spectral profiles. The spectra displayed here are processed with $\text{LB} = 0.3$ Hz exponential apodization. The complete chemical shifts assignments are listed in Table S1 in the Supporting Information. It should be noted that the lipid resonances shown in the HR-MACS spectrum overlap with small background signals from the resonator, see Figure S1 in the Supporting Information.

for identifying the metabolic variations between the two strains. Principal component analysis (PCA) of the full data set has indicated one outlier (Figure S3b in the Supporting Information) for which the corresponding ^1H NMR spectrum reveals unknown impurities in the sample. This data was thus discarded for further multivariate analysis. The PCA score plot also provides a visual discrimination pattern between the two

strains, with the wild-type strain samples closely clustered at the center and the *slcf-1* mutant samples scattered in the score plot. Figure 3 shows the supervised statistical analysis using OPLS-DA, in which the score plot (Figure 3a) displays a remarkably clear discrimination between the two strains. Interestingly, it also shows a greater metabolic variation (i.e., along the orthogonal component t_{orth}) within the *slcf-1* mutants, agreeing

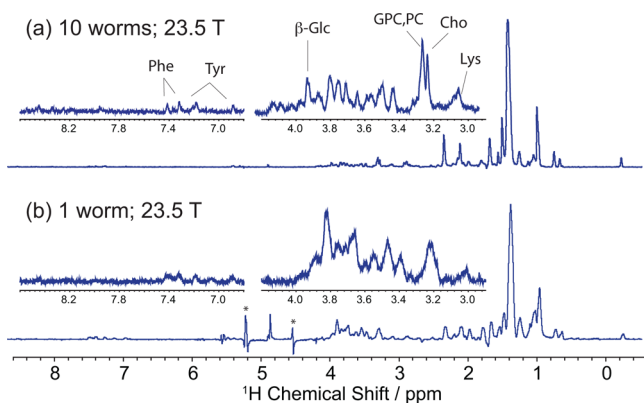


Figure 2. ^1H NMR spectra of (a) 10 worms and (b) 1 worm. The spectra were acquired at 23.3 T with a 3.2 mm CP-MAS probe. Spectra are processed with $\text{LB} = 0.3$ Hz exponential apodization.

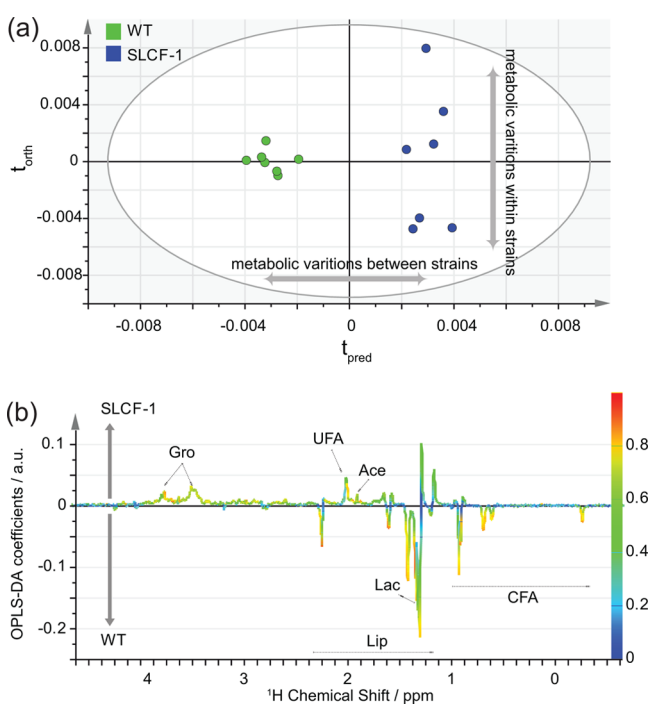


Figure 3. Multivariate discrimination model for wild-type and *slcf-1* strain worms from ^1H NMR profiles: (a) OPLS-DA score plot and (b) the corresponding loading plot. The model is obtained using one predictive and three orthogonal components and shows an excellent differentiation between the strain worms with goodness-of-fit parameters: $Q^2 = 0.784$, $R^2Y(\text{cum}) = 0.964$, and $R^2X(\text{cum}) = 0.889$.

with the observed scatter pattern in the PCA score plot. This may suggest that the *slcf-1* worms sample consist of a greater interindividual variability in metabolite. Further investigations are underway to understand the large metabolic variation within the mutant strains. The corresponding loadings plot (Figure 3b) illustrates metabolites associated with the separation in the score plot. Positive lines are associated with metabolites in higher concentration for the *slcf-1* mutants as compared to wild-type worms, while negative peaks represent metabolites in lower concentration for the long-lived mutants. The colors in the observed lines correspond to the correlation of the individual metabolites variation to the multivariate discrimination.

DISCUSSION

The above results have demonstrated the possibility of NMR-based metabolomics studies of small quantity *C. elegans* using HR-MACS. The beneficial factors besides its enhanced mass-sensitivity and high spectral resolutions are described below.

Simplified Sample Preparation. Often in a metabolomics NMR study, one requires multisampling, collecting data of multiple samples from the same origin. Let us consider the above discrimination study involving two different *C. elegans* strains. To minimize analytical errors, seven replicate samples are used for the metabolomics investigations. With HR-MAS, it would require a worm population of 1000 for each NMR acquisition, which means a total of 14,000 worms ($1000 \text{ worms} \times 7 \text{ samples} \times 2 \text{ groups}$) for the study. Such large sample pools involve labor-intensive preparation, requiring 140 agar plates for the worm cultivations (i.e., about 100 worms per plate), and clearly limits the size of accessible studies. On the other hand, a total of only 1,400 worms (14 plates) are needed for an equivalent study with HR-MACS (100 worms for each of the 14 NMR data). This dramatic reduction in the sampling pool not only reduces the cost of labor, time, and consumables, but it opens new possibilities for large-scale metabolomics analysis of *C. elegans*, for example, in the context of functional genomics investigations for which a large number of *C. elegans* mutants should be studied.

Enhanced Sample Selectivity. Large volume HR-MAS studies rely on large populations of worms build up on population sampling to average out the interindividual variability and define global metabolomics phenotypes associated with a nematode strain. Significantly, the possibility to study few worms offers new avenues to explore the phenotypic diversity linked to environmental/epigenetic regulation among isogenic worms from the same strain. Also, preparation of a small sample pool allows individual screening of the worms and selection of a desired morphologic or behavioral phenotype, therefore potentially bringing new metabolic insights to the heterogeneous response of a population to a given perturbation (mutation, drug treatment, etc.).

Simple Sample Filling Procedure. It is acknowledged that sample filling in a micrometer size capillary (i.e., HR-MACS) can be a strenuous task especially with adhesive tissues; however, in the case of *C. elegans* worms, it involves a straightforward filling procedure by simply transferring the worms into the capillary along with D_2O solution using a micropipet.

Minimal Sample Destruction. The sample interference in HR-MACS detection is minimal as compared to HR-MAS or to mass spectrometry that requires a careful design extraction protocol.²⁰ This is because the centrifugal force exerted upon the worms is greatly reduced by the slow sample spinning experiment and the small diameter sample capillary. The force is estimated to be in the order of 10^{-3} N. This is negligible as compared to the ~ 15 N exerted upon the worms under HR-MAS acquisition with a 3500 Hz sample spinning frequency. In fact, physical degradation of the worms is evident under microscopy after an acquisition with HR-MAS. Blaise et al.¹⁰ have reported spectral evidence of cellular compartment rupture in the nematodes after 4 h of NMR acquisition at moderate sample spinning (3500 Hz). Sample heating is another issue especially for sensitive samples such as living organisms. Friction (fast spinning), radio frequency (high rf

power), and electric field (ionic sample) are considered the main sources of heating in the case of HR-MAS experiments. However, from previous assessments,^{19,25,26} we have found that the presence of eddy currents in the wire, originating from the μ coil spinning in a magnetic field, is the main contribution to heating in the case of HR-MACS. It is estimated that the heating should not exceed 0.05 °C from a 550- μ m HR-MACS spinning at 350 Hz inside 23.5 T. Thus, slow spinning frequency <500 Hz is performed in HR-MACS experiments to minimize this eddy currents effect.

Great Versatility. The HR-MACS resonator can be readily adapted to commercial MAS probes, including the HR-MAS probe, without modifications. Moreover, the resonator can be easily adjusted to any frequency offering a wide nuclei range of NMR detections at any B_0 fields.

The above beneficial factors from HR-MACS offer a promising microprobe to carry out NMR-based metabolomics studies of *C. elegans* or other submillimeter size organisms. To our knowledge, there are no other analytical techniques capable of offering metabolic profiling with such small-scale worm population without damaging or interfering the sample anatomy.

There are however a few remaining weaknesses even with using HR-MACS, the most obvious being the low detection sensitivity for small sample volume, which is intrinsic to NMR. Even though HR-MACS provides excellent mass-sensitivity enhancement, the absolute abundance of metabolites in a nanoliter volume is low; thus, longer data acquisition is required to detect low concentration metabolites. Another downside is the slow sample spinning, despite the fact that it enhances the spectral resolution and minimizes the sample destruction,¹⁹ the overall signal intensity is dissipated throughout observable spinning-sideband manifolds, reducing the intrinsic intensity of the isotropic resonances.²⁷ However, such loss is minimal compared to the sensitivity gain from the B_1/ρ efficiency. This is because the sideband manifolds are generally small for semisolid samples like worms. The above issues could be eliminated, or minimized, with automated microfabrication of HR-MACS²⁸ or a standalone HR-MAS NMR microprobe. Furthermore, the intrinsic low sensitivity could be improved by coupling with other sensitivity enhancement techniques such as dissolution DNP²⁹ and cryogenic MAS probes.

CONCLUSIONS

The results shown here highlight the potential of a novel means of addressing the current limitations of NMR-based metabolomics of intact millimeter size organisms. We have demonstrated the ability of NMR metabolic profiling and discrimination analysis of finite *C. elegans* nematodes, with no more than 100 individuals. These results are an important advancement in μ NMR application of magic angle coil spinning (MACS) to metabolomics. It offers a dramatic reduction of labor-intensive sample preparations and the possibility of high-throughput organism screening. Moreover, it can potentially offer a first-order individual screening of specific phenotype nematodes, which it is not possible with large sample analysis. The results presented here pave ways to a new platform of NMR-based metabolomics of *C. elegans*. Advancing the development of microtechnology in MAS will no doubt broaden the feasibility of routinely screening in small organisms, intact whole cells and biopsies, and will certainly enhance the impact in metabolomics applications to a vast

biological spectrum such as biomarker discovery, toxicology screening, and clinical study.

ASSOCIATED CONTENT

Supporting Information

All identifiable metabolites from HR-MAS and HR-MACS spectra (in Figure 1) summarized in Table S1; ^1H background signal in Figure S1; description of a sample-exchangeable HR-MACS resonator in Figure S2; ^1H HR-MACS NMR data for the discrimination study in Figure S3 with PCA analysis. This material is available free of charge via the Internet at <http://pubs.acs.org>.

AUTHOR INFORMATION

Corresponding Authors

*E-mail: alan.wong@cea.fr.

*E-mail: dimitrios.sakellariou@cea.fr.

Present Address

^{||}X.L.: Chinese Academy of Sciences, Institute of Electrical Engineering, 6 Beiertiao, Zhongguancun, 100190, Beijing, China.

Author Contributions

A.W., B.E.-H., and D.S. designed the study; A.W., B.E.-H., F.S., X.L., and L.M. performed the study; A.W., B.E.-H., and F.S. performed the analysis; A.W., B.E.-H., F.S., and D.S. wrote the paper.

Notes

The authors declare no competing financial interest.

ACKNOWLEDGMENTS

We would like to thank the financial support from the French National Research Agency under Grant ANR33HRMACSZ, the European Research Council under the European Community's Seventh Framework Programme, ERC Grant Agreement 205119. We are also grateful for the Très Grandes Infrastructures de Recherche (TGIR-RMN Grant FR3050) in France for providing access to the high field NMR facility in Lyon and the traveling funds. We would like to acknowledge Dr. David Gajan (Lyon, France) for his assistance on the 1000 MHz experiments, Mr. Angelo Guiga (Saclay, France) for fabricating the Kel-F inserts, and Mr. Rech Alexandre (Lyon, France) for his assistance on the assessment of the ^1H background signals of HR-MACS.

REFERENCES

- (1) Dunn, W. B.; Ellis, D. I. *Trends Anal. Chem.* **2005**, *24*, 285–294.
- (2) Lindon, J. C.; Holmes, E.; Nicholson, J. K. *Anal. Chem.* **2003**, *75*, 384A–391A.
- (3) Reo, N. V. *Drug Chem. Toxicol.* **2002**, *25*, 375–382.
- (4) Beckonert, O.; Coen, M.; Keun, H. C.; Wang, Y.; Ebbels, T. M. D.; Holmes, E.; Lindon, J. C.; Nicholson, J. K. *Nat. Protoc.* **2010**, *5*, 1019–1032.
- (5) Sitter, B.; Bateh, T. F.; Tessem, M.-B.; Gribbestad, I. S. *Prog. Nucl. Magn. Reson.* **2009**, *54*, 239–254.
- (6) Lindon, J. C.; Beckonert, O. P.; Holmes, E.; Nicholson, J. K. *Prog. Nucl. Magn. Reson.* **2009**, *55*, 79–100.
- (7) Nicholson, J. K.; Holmes, E.; Kinross, J. M.; Darzi, A. W.; Takats, Z.; Lindon, J. C. *Nature* **2012**, *491*, 384–392.
- (8) Piotto, M.; Moussallieh, F. M.; Neuville, A.; Bellocq, J. P.; Elbayed, K.; Namer, I. J. *J. Med. Case Rep.* **2012**, *6*, 22.
- (9) Blaise, B. J.; Giacomotto, J.; Elena, B.; Dumas, M.-E.; Toulhoat, P.; Ségalat, L.; Emsley, L. *Proc. Natl. Acad. Sci. U.S.A.* **2007**, *104*, 19808–19812.

- (10) Blaise, B. J.; Giacomotto, J.; Triba, M. N.; Toulhoat, P.; Piotto, M.; Emsley, L.; Ségalat, L.; Dumas, M. E.; Elena, B. J. *Proteome Res.* **2009**, *8*, 2542–2550.
- (11) Pontoizeau, C.; Mouchiroud, L.; Molin, L.; Mergoud-dit-Lamarche, A.; Dalliere, N.; Toulhoat, P.; Elena-Herrmann, B.; Solari, F. J. *Proteome Res.* **2014**, DOI: 10.1021/pr5000686.
- (12) Hoult, D. I.; Richards, R. E. *J. Magn. Reson.* **1976**, *24*, 71–85.
- (13) Bhattacharya, A. *Nature* **2010**, *463*, 605–606.
- (14) Aramini, J. M.; Rossi, P.; Anklin, C.; Xiao, R.; Montelione, G. T. *Nat. Methods* **2007**, *4*, 491–493.
- (15) Janssen, H.; Brinkmann, A.; van Eck, E. R. H.; van Bentum, J. M.; Kentgens, A. P. M. *J. Am. Chem. Soc.* **2006**, *128*, 8722–8723.
- (16) A μ MAS probe released in April 2012 by JEOL Resonance, Inc.
- (17) Sakellariou, D.; Le Goff, G.; Jacquinet, J.-F. *Nature* **2007**, *447*, 694–697.
- (18) Wong, A.; Jiménez, B.; Li, X.; Homes, E.; Nicholsson, J. K.; Linton, J. C.; Sakellariou, D. *Anal. Chem.* **2012**, *84*, 3843–3848.
- (19) Wong, A.; Li, X.; Sakellariou, D. *Anal. Chem.* **2013**, *85*, 2021–2026.
- (20) Geier, F. M.; Want, E. J.; Leroi, A. M.; Bundy, J. G. *Anal. Chem.* **2011**, *83*, 3730–3736.
- (21) Castro, C.; Krumsiek, J.; Lehrbach, N. J.; Murfitt, S. A.; Miska, E. A.; Griffin, J. L. *Mol. Biol. Syst.* **2013**, *9*, 1632–1642.
- (22) Mouchiroud, L.; Molin, L.; Kasturi, P.; Triba, M. N.; Dumas, M. E.; Wilson, M. C.; Halestrap, A. P.; Roussei, D.; Masse, I.; Dallière, N.; Ségalat, L.; Billaud, M.; Solari, F. *Aging Cell* **2011**, *10*, 39–54.
- (23) Antzutkin, O. N.; Shekar, S. C.; Levitt, M. H. *J. Magn. Reson. A* **1995**, *115*, 7–19.
- (24) Peti, W.; Norcross, J.; Eldridge, G.; O'Neil-Johnson, M. *J. Am. Chem. Soc.* **2004**, *126*, 5873–5878.
- (25) Aguiar, P. M.; Jacquinet, J.-F.; Sakellariou, D. *J. Magn. Reson.* **2009**, *200*, 6–14.
- (26) Aubert, G.; Jacquinet, J.-F.; Sakellariou, D. *J. Chem. Phys.* **2012**, *137*, 154201.
- (27) Renault, M.; Shintu, L.; Piotto, M.; Caldarelli, S. *Sci. Rep.* **2013**, *3*, 3349.
- (28) Badilita, V.; Fassbender, B.; Kratt, K.; Wong, A.; Bonhomme, C.; Sakellariou, D.; Korvink, J. G.; Walrabe, U. *PLoS One* **2012**, *7*, e42848.
- (29) Nelson, S. J.; Kurhanewick, J.; Vigneron, D. B.; Larson, P. E. Z.; Harzstark, A. L.; Ferrone, M.; van Crieking, M.; Chang, J. W.; Bok, R.; Park, I.; Reed, G.; Carvajal, L.; Small, E. J.; Munster, P.; Weinberg, V. K.; Ardenkjaer-Larsen, J. H.; Chen, A. P.; Hurd, R. E.; Odegardstuen, L.-I.; Robb, F. J.; Tropp, J.; Murray, J. A. *Sci. Transl. Med.* **2013**, *5*, 198ra108.

Supporting Information

μ HR-MAS NMR Spectroscopy for Metabolic Phenotyping of *Caenorhabditis Elegans*

Alan Wong^{a*}, Xiaonan Li^{a,d}, Laurent Molin^b, Florence Solari^b, Bénédicte Elena-Herrmann^c, Dimitris Sakellariou^{a*}

^a CEA Saclay, DSM, IRAMIS, UMR CEA/CNRS 3299 – NIMBE, Laboratoire Structure et Dynamique par Résonance Magnétique, F-91191, Gif-sur-Yvette Cedex, France

^b Centre de Génétique et de Physiologie Moléculaires et Cellulaires, UMR CNRS 5534, Université Claude Bernard Lyon 1, Bâtiment Gregor Mendel, 16 rue Raphaël Dubois, F-69622 Villeurbanne Cedex, France

^c Centre de RMN à très hauts champs, Institut des Sciences Analytiques, CNRS/ ENS Lyon / UCB Lyon-1, Université de Lyon, 5 rue de la Doua, 69100 Villeurbanne, France

^d current address: Chinese Academy of Sciences, Institute of Electrical Engineering, 6 Beiertiao, Zhongguancun, 100190, Beijing, China

Corresponding author: (AW) alan.wong@cea.fr

Table S1 Metabolite assignments	S2
Figure S1 ¹ H background signal	S4
Figure S2 Description of sample-exchangeable HR-MACS resonator	S5
Figure S3 ¹ H HR-MACS dataset and PCA of the discrimination study	S6

Table S1. NMR metabolic profiling of *C. elegans* from the ¹H-detected HR-MACS and HR-MAS NMR spectra shown in Figure 1 in the main text.

Metabolite	abbreviation	¹ H shift (multiplicity) ^a	detection ^b
acetate	Ace	1.91(s)	M,m
acetoacetate	Aca	3.44(s)	M
adenine	Ade	8.18(s), 8.22(s)	M
adenosine	Ads	4.43(m), 6.10(d), 8.25(s), 8.34(s)	M
alanine	Ala	1.47(d), 3.77(q)	M,m
β-alanine	β-Ala	2.55(t), 3.18(t)	M
γ-aminobutyrate	GABA	1.89(m), 3.01(m)	M,m
arginine	Arg	1.64(m), 1.72(m), 1.89(m), 1.91(m), 3.24 (m), 3.76(t)	M,m
asparagine	Asn	2.85(dd), 2.94(dd), 4.00(dd)	M
<i>aspartate</i>	<i>Asp</i>	<i>2.67(d), 2.80(dd), 3.89(dd)</i>	<i>M</i>
ATP	ATP	4.77(m), 6.14(d), 8.25(s), 8.50(s)	M
betaine	Bet	3.26(s), 3.90 (s)	M,m
CFA	CFA	−0.32(m), 0.58(m), 0.66(m), 1.17(m), 1.41(m)	M,m
choline	Cho	3.20(s), 3.51(m), 4.06(m)	M,m
<i>creatinine</i>	<i>Cre</i>	<i>3.03(s), 4.04(s)</i>	<i>M,m</i>
cystathionine	Cyn	2.15(m), 2.72(m), 3.07(m), 3.84(dd), 3.93(dd)	M
dihydrouracil	Dhu	2.66(t), 3.45(t)	M
formate	For	8.44(s)	M,m
β-galactose	Gal	3.64(dd), 4.59(d)	M
α-glucose	α-Glc	3.40(t), 3.54(t), 3.71(dd), 3.81(m), 3.92(m), 5.22(d)	M
β-glucose	β-Glc	3.24(m), 3.39(t), 3.47(dd), 3.89(dd), 4.64(d)	M,m
glutamate	Glu	2.12(m), 2.34(m), 3.76(dd)	M,m
glutamine	Gln	2.13(m), 2.44(m), 3.76(t)	M,m
Glutathione	GSSG	2.16(m), 2.53(m), 2.94(m), 3.77(m)	M
GPC	GPC	3.22(s), 3.61(dd), 3.66(m), 3.87(m), 4.31(m)	M,m
glycerol	Gro	3.55(dd), 3.64(dd), 3.86(m)	M
glycine	Gly	3.55(s)	M,m
guanosine	Guo	4.22(q), 4.40(m), 5.90(d), 8.00(s)	M
indole	Ind	6.60(d), 7.25(m), 7.54(d), 7.70(d),	M
inosine	Ins	3.84 (dd), 3.91 (dd), 4.22(m), 4.43(m), 6.10(d), 8.22(s), 8.34(s)	M,m
isoleucine	Ile	0.93(t), 1.00(d), 3.66(d)	M,m
lactate	Lac	1.32(d), 4.11 (q)	M,m
leucine	Leu	0.94(d), 0.96(d), 1.70(m), 3.72(m)	M,m
Lipids	Lip	0.88(m), 0.89(m), 0.90(m)*, 1.30(m)*, 1.59(m)*, 2.06(m)*, 2.26(m)*, 2.76(m), 2.80(m), 4.09(m), 4.29(m),	M,m
lysine	Lys	1.71 (m), 1.89(m), 3.01(t), 3.75(t)	M,m
methanol	MeOH	3.35(s)	M,m
methionine	Met	2.11(m), 2.12(s), 2.63(t)	M,m
<i>myo-inositol</i>	<i>Myo-Ins</i>	<i>3.28(m), 3.53(m), 3.62(m), 4.06(m)</i>	<i>M,m</i>
N6-acetyllysine	Nal	1.53(m), 1.86(m), 1.98(s), 3.18(m), 3.74(m), 7.96(s)	M
nicotinate	Nia	7.53(dd), 8.25(m), 8.61(dd), 8.94(d)	M
ornithine	Orn	3.05(t)	M,m
phenylalanine	Phe	3.12(dd), 3.27(dd), 3.99(dd), 7.36(m), 7.41(m)	M,m
phosphocholine	PC	3.22(s), 3.57(m), 4.19(m)	M,m
<i>2-phosphoglycerate</i>	<i>2PG</i>	<i>3.81(dd), 3.90(dd), 4.48(m)</i>	<i>M</i>
serine	Ser	3.83(dd), 3.96(m)	M
sucrose	Suc	3.46(t), 3.67(m), 3.76(m), 3.82(m), 3.88(m), 4.04(t), 4.21(d), 5.41(d)	M,m
trehalose	Tre	3.64(dd), 3.82(m), 5.18(d)	M
threonine	Thr	1.32(d), 3.58(d), 4.25(m)	M,m
tyrosine	Tyr	3.04(dd), 3.19(dd), 3.94(dd), 6.88(d), 7.18(d)	M,m
unsaturated lipids	UFA	2.03(m), 2.84(m), 5.32(m)	M,m
Uracil	Ura	5.79(d), 7.52(d)	M
Uridine	Urd	4.22(t), 4.34(t), 5.89(d), 5.91(d), 7.88(d)	M
Valine	Val	0.98(d), 1.04(d), 3.60(d)	M,m

CFA = cyclopropane fatty acids; GPC = glycerophosphocholine

a) The assignments are based on proprietary (Chenomx NMR suite, Chenomx Inc., Edmonton, Canada) and academic (HMDB¹) databases, as well as earlier literatures.^{2,3} Abbreviations: s = singlet; d = doublet; dd = doublet of doublets; t = triplet; m = multiplet. The asterisk * indicates an overlapping signal with a background signal (see Figure S1)

b) M = HR-MAS; m = HR-MACS; Italics represents for the presence of strong overlap with other metabolites.

- (1) Wishart, D. S.; Knox, C.; Guo, A. C.; Eisner, R.; Young, N.; Gautam, B.; Hau, D. D.; Psychogios, N.; Dong, E.; Bouatra, S.; Mandal, R.; Sinelnikov, I.; Xia, J.; Cruz, J. A. ; Lim, E.; Sobsey, C. A.; Shrivastava, S.; Huang, P.; Liu, P.; Fang, L.; Peng, J.; Fradette, R.; Cheng, D.; Tzur, D.; Clements, M.; Lewis, A.; De Souza, A.; Zuniga, A.; Dawe, M.; Xiong, Y.; Clive, D.; Greiner, R.; Nazyrova, A.; Shaykhutdinov, R.; Li, L.; Vogel, H. J.; Forsythe I. *Nucleic. Acids Res.* **2009**, *37*, D603–D610.
- (2) Blaise, B. J.; Giacomotto, J. Elena, B.; Dumas, M-E.; Toulhoat, P.; Ségalat, L.; Emsley, L. *Proc. Nat. Acad. Sci.* **2007**, *104*, 19808–19812.
- (3) Nicholson, J. K.; Foxall, P. J. D.; Spraul, M.; Farrant, R. D.; Lindon, J. C. *Anal. Chem.* **1995**, *67*, 793–811.

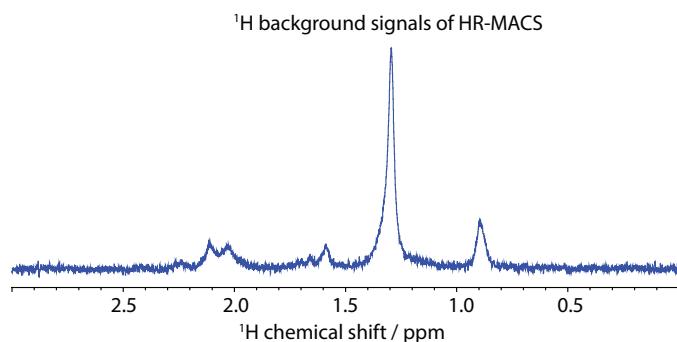


Figure S1. ^1H HR-MACS background signals. It acquired with a $2\ \mu\text{M}$ sucrose/ D_2O solution with an sample-exchangeable $840\text{-}\mu\text{m}$ HR-MACS resonator (more description can be found in Figure S2) at 11.75 T spinning at 300 Hz. Water-suppression 8-step PASS sequence was performed to acquire water- and sideband-free spectra. The total acquisition time is 132 minutes comparable to that of *C. elegans* in the text. For clarity, the figure shows the expansion region (0 – 3 ppm). The observed background signals correspond to the aliphatic protons of the glue and/or the epoxy in HR-MACS, and display a similar profile as the lipid resonances in *C. elegans*. The signals do not interfere the neighboring metabolite resonances such as lactate, alanine and valine at 1.33, 1.47 and 1.04 ppm, respectively. Indeed well resolved doublets are observed.

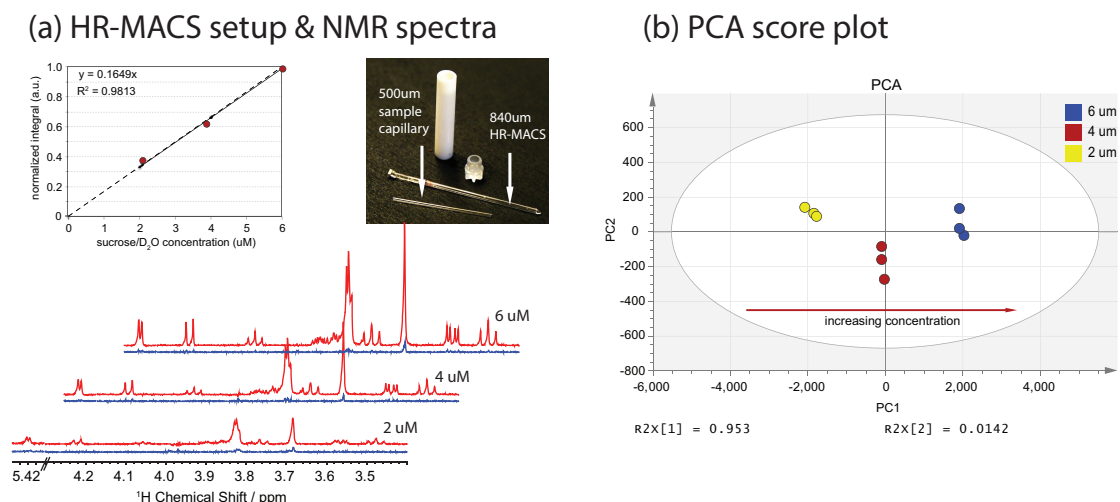


Figure S2. To ensure the spectral reproducibility ‘one’ 840-μm HR-MACS resonator is used for the replicate samples, in which the resonator is permanently fixed inside a 4-mm MAS rotor, allowing for a freely sample screening with a sample-exchangeable 550-μm capillary. To demonstrate the spectral data reproducibility, we recorded ¹H HR-MACS NMR spectra of three different concentrations of sucrose/D₂O solution: 2, 4 and 6 μM with a total detection volume of 200 nL. Triplicate samples were recorded for each concentration. All spectra were recorded under the same experimental conditions at 11.75 T with a MAS frequency at 300 Hz. Water-suppression 8-step PASS sequence was performed to acquire water- and sideband-free spectra. Prior to multivariate analysis, the spectra were phased and baseline-corrected without apodization using the Bruker interface Topspin 3.0. The spectra were bucketed by 0.001 ppm interval and normalized by the total integration values over the spectral region of 3.4 – 5.5 ppm, excluding the water region (4.70 – 4.85 ppm). These spectral bucketing and normalization were done using MestReNova 8.1. Principal component analysis (PCA) was performed using the SIMCA algorithms in SIMCA-P 13.

(a) The red spectrum represents the mean spectrum for each concentration, and the blue corresponds the standard deviation spectrum. The insert photo displays the sample-exchangeable HR-MACS setup. The plot shows the correlation between the total spectral integral of the mean spectra with the corresponding concentrations. The dotted line is the expected correlation. (b) The PCA score plot showing the quality of the sub-spectra ($R^2X(\text{cum}) = 0.967$; $Q^2(\text{cum}) = 0.938$). Both the tightly packed cluster in PCA and the small signal in the standard deviation spectra validate the data reproducibility with the sample-exchangeable HR-MACS setup.

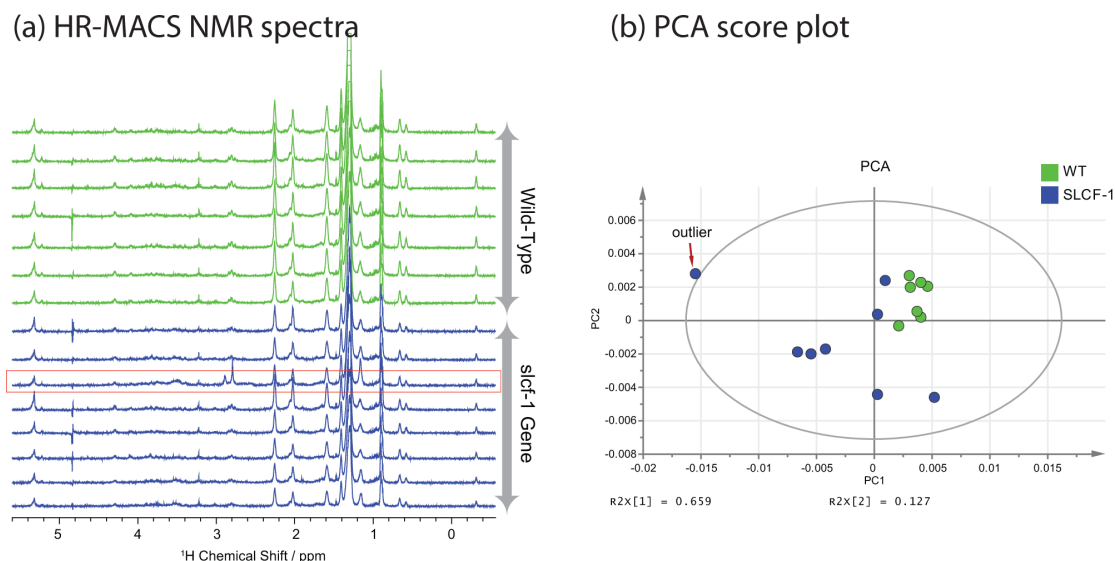


Figure S3. ^1H HR-MACS NMR dataset for the discrimination analysis of two *C. elegans* strains.

(a) ^1H HR-MACS NMR sampling of wild-type and *slcf-1* strains. The spectra were acquired with 50 ± 20 worms using the sample-exchangeable resonator at 18.8 T spinning at 300 Hz. The acquisition time for each spectrum was about 2.5 hr. A 4-fold mass-sensitivity enhancement ($B_1^{\text{HRMACS}}/B_1^{\text{MAS}} = 4$) is found with the sample-exchangeable resonator. It is to note that this 840- μm resonator sacrifices the sensitivity through the sample-filling factor and the B_1/i efficiency (*i.e.* larger μcoil) compare to the HR-MACS used in Figures 1, in which the sample is directly placed inside the 550- μm resonator with a near optimal filling factor and better B_1/i efficiency. Consequently, higher worm population is required to compensate the sensitivity lost. Table 1 in the main text details the comparison in NMR performances with other resonators used in the study.

An exponential apodization function corresponding to a line-broadening of 0.7 Hz was used before Fourier transformation. Manual first-order phase correction, and baseline adjustment were applied on the spectra using Topspin 3.0 (Bruker Biospin GmbH, Rheinstetten, Germany).

(b) The PCA score plot of all NMR spectra showing a differentiation of metabolic variations for both strains: wild-type (green dot) and *slcf-1* (blue dot), with $R^2X(\text{cum}) = 0.964$; $Q^2(\text{cum}) = 0.8$. PCA also offers to check the homogeneity of the NMR dataset and, if appropriate, subsequently exclude any outliers. In this case, one outlier is found in which the NMR spectrum, the red-box in (a), reveals unknown impurities in the region of about 2.8 and 3.5 ppm.